THE JOURNAL OF PHYSICAL CHEMISTRY A
A JOURNAL OF THE AMERICAN CHEMICAL SOCIETY

pubs.acs.org/JPCA Article

Thermodynamics of the van der Waals Dimers of O_2, N_2 and the Heterodimer $(N_2)(O_2)$ and Their Presence in Earth's Atmosphere

Arthur M. Halpern*

Cite This: https://doi.org/10.1021/acs.jpca.3c04809 Read Online

ACCESS | Metrics & More | Article Recommendations | Supporting Information

ABSTRACT: The dimerization thermodynamics of N_2 and O_2, the principal components of Earth's atmosphere, have been determined from the respective second virial coefficients of the bound and metastable dimers calculated using the method of Stogryn and Hirschfelder that utilizes the Lennard-Jones (LJ) potential to account for intermolecular interactions. In addition, the thermodynamic properties of the heterodimer $(N_2)(O_2)$ have been obtained using the same approach, employing combining rules to construct the LJ potential. Thus, K_{eq}, ΔH, and ΔS for the three dimers are reported between 80−120 K. Over this temperature range, the ranking of K_{eq} is $(N_2)(O_2) > (O_2)(O_2) > (N_2)(N_2)$. The same trend is found for the exoethalpicity of dimer formation. For example, at 100 K, the K_{eq} values are, respectively, 0.0406(14), 0.0215(5), and 0.0181(10), and the corresponding ΔH values are −2401(5), −2344(7), and −2279(1) J/mol. The mole fraction composition of the dimers in the atmosphere was calculated for altitudes up to 20 km. These calculations show that in the troposphere and the lower stratosphere (up to 20 km), the three dimers rank fifth to seventh in abundance, between CO_2 and Ne. In this region, the average mole fractions of $(N_2)(N_2)$, $(O_2)(O_2)$, and $(N_2)(O_2)$ are calculated to be $3.4(2) \times 10^{-4}$, $2.80(9) \times 10^{-5}$, and $1.95(7) \times 10^{-4}$, respectively.

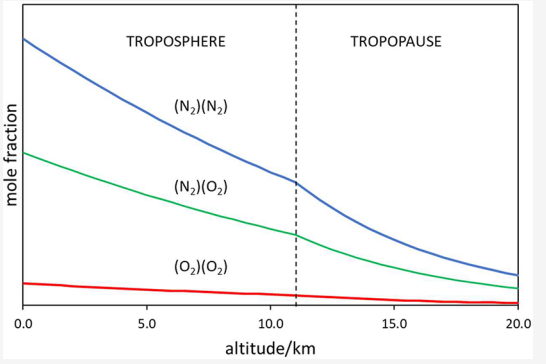

INTRODUCTION

The term "van der Waals molecule" was used by Ewing in 1972 to describe the noncovalently bound dimers of Ar, H_2, O_2, and others.[1] That term has been widely used since then to characterize or categorize many weakly bound association complexes. Although a number of studies have been reported concerning the nature of the interactions between the components, few have dealt with the equilibrium thermodynamic properties of van der Waals dimers and trimers. In recent publications, such information has been obtained from the equation of state (EOS) of the rare gases He − Xe and for 10 nonpolar molecules ranging from H_2 to $C(CH_3)_4$.[2−6] Since the thermodynamic properties of heterodimer formation cannot be obtained from the EOS-based method that can be employed for the homodimers, we sought an approach that could be applied to all three dimers, $(N_2)(N_2)$, $(O_2)(O_2)$, and $(N_2)(O_2)$. Such calculations would provide consistency to the results thus obtained.

The present work describes studies relating to the dimers of N_2, O_2, and the heterodimer $(N_2)(O_2)$ using a different approach and reports their equilibrium constants and thermodynamic properties in two temperature ranges, 80−120 and 217−288 K, the latter range being relevant to Earth's atmosphere up to 20 km.

A number of ab initio studies have been reported on the pair potentials and potential energy surfaces of N_2 and O_2 dimers.[7−22] Far fewer describe calculations of the $(N_2)(O_2)$ heterodimer.[19−22] Calculations indicate that there are several structural forms of these dimers, as shown in Figure 1. There are two T structures for $(N_2)(O_2)$ in which the O_2 or N_2 moiety is positioned along the C_2 symmetry axis. These structural forms are located on the hypersurfaces of the respective dimers and are relevant to the macroscopic equilibrium thermodynamic properties of the gases.

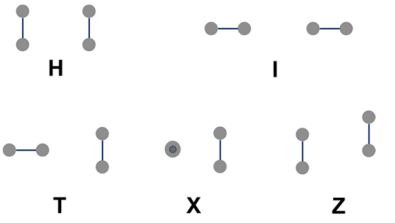

Figure 1. Previously reported dimer structures.[11,16,22] In the case of $(N_2)(O_2)$, there are two T structures, T1 and T2, in which the O_2 or N_2 moiety lies along the symmetry axis, respectively.

Received: July 17, 2023
Revised: October 19, 2023
Accepted: November 8, 2023

A 1994 paper by Slanina et al. presented the atmospheric altitude profile of $(N_2)(N_2)$, $(O_2)(O_2)$, and $(N_2)(O_2)$ based on mp4/6-31+g* calculations with and without counterpoise adjustments.[20] Considering that N_2 and O_2 are the predominant components of the atmosphere and the relatively high collision frequency between these molecules, it is important to reconsider the atmospheric composition of these three dimers from calculations based on the real gas properties of N_2 and O_2 under equilibrium conditions. That is the principal aim of this report.

Method, Assumptions, and Reliability. Stogryn and Hirschfelder (S−H) provided such an opportunity.[23,24] That work describes the calculation of the second virial coefficient (SVC) of a gas that relies on the centrosymmetric Lennard-Jones (LJ) potential to account for intermolecular interactions. Of particular importance is that the SVC is obtained by considering three components, i.e., interactions that lead to the formation of bound molecule-pairs (dimers), quasibound (metastable) pairs, and pairwise collisions that do not produce dimers. It should be noted that calculations in the present work are based on the corrected S−H expression for the reduced SVC for the metastable dimers.[24] The SVC thus obtained is used to calculate the monomer−dimer equilibrium constant described by

$$2M \rightleftharpoons DK_{eq} \tag{1}$$

in which M and D are the monomer (N_2 or/and O_2) and dimer, respectively. For the calculation of K_{eq} (at a given temperature), one needs only the parameters σ and ε of the LJ potential

$$V(r) = 4\varepsilon\left[\left(\frac{\sigma}{r}\right)^{12} - \left(\frac{\sigma}{r}\right)^{6}\right] \tag{2}$$

in which r is the intermolecular separation, ε is the potential well depth, and σ is the finite value of r at which $V(r) = 0$.

In our study, the S−H method was also used to calculate the equilibrium thermodynamic properties of the heterodimer $(N_2)(O_2)$ by employing combining rules to obtain σ and ε for the mixed dimer from the parameters of the respective monomers N_2 and O_2, assuming that this potential describes pairwise interactions between the N_2 and the O_2 monomers.

A chief advantage of the S−H method is that the dimerization thermodynamics of any pair of entities can be studied as long as the LJ parameters are known. However, as pointed out by Frurip et al.,[25] the method of obtaining K_{eq} from SVCs relies on the utilization of an "excluded volume," which incurs a degree of "ambiguity." But in the S−H calculation, this excluded volume is directly related to the LJ σ parameter; moreover, as pointed out in ref 23, the computational method relates K_{eq} to the intermolecular potential "without the introduction of any empirical concepts." The method also assumes that the fugacity coefficients of the monomer and dimer are equal to unity.

An important aspect of this method is that the LJ parameters used to calculate K_{eq} depend upon the method used to obtain them (e.g., transport properties, SVCs, simulations, etc.). In order to assess the effect of the choice of LJ parameters on the calculated value of K_{eq} and related thermochemical properties, we performed calculations using two sets of LJ parameters for N_2 and O_2 and by applying three combing rules to those parameter sets to obtain the parameters used in the S−H calculations for the heterodimer equilibrium

$$N_2 + O_2 \rightleftharpoons (N_2)(O_2)K_{eq} \tag{3}$$

Note that K_{eq} is used generically throughout this work to denote the dimerization equilibrium constant and associated thermophysical quantities.

Thus, two different sets of LJ parameters were used for the calculation of the thermodynamic properties of each of the homodimers and six for the heterodimer. In this way, the degree of systematic uncertainty in K_{eq} values can be estimated from these calculations, as discussed in the next section. One set of parameters was obtained from the respective SVCs[26] of N_2 and O_2, and the other set from molecular dynamics calculations.[27] The LJ parameters used and the combining rules employed[28,29] in this work are shown in the Supporting Information (SI).

The intrinsic uncertainty associated with the S−H method and its effect on the calculated results are difficult to assess. However, in an attempt to benchmark such calculations and to establish a degree of reliability, we sought to compare the calculated K_{eq} values with those obtained experimentally. Unfortunately, there are few opportunities for such a comparison. However, one example is provided by the quantitative mass spectrometric detection of argon dimer number densities in a jet-expanded molecular beam study, as reported by Milne et al.[30,31] Their results permit the calculation of K_{eq} at four temperatures under the assumption that the population of Ar_2 detected represents the equilibrium distribution of dimers at the temperature of the pre-expanded gas. Table 1 shows the results of the S−H calculations of K_{eq} for Ar dimer formation, along with the experimental values reported in refs 30 and 31.

Table 1. K_{eq} Values for Argon Dimerization Calculated Using the S−H Method and Obtained from Mass Spectrometric Studies

T/K	K_{eq} calculated[a]	K_{eq} experimental[b]
118	1.2×10^{-2}	1.2×10^{-2}
167	4.5×10^{-3}	4.1×10^{-3}
220	2.2×10^{-3}	2.2×10^{-3}
300	1.0×10^{-3}	8.0×10^{-4}; 7.1×10^{-4}[c]

[a]S−H method (ref 23) using the average of the two LJ parameter sets described in the SI. [b]Interpreted from Figure 1 of ref 30. [c]Reference 31.

The good agreement between the calculated and experimental values of K_D seen in Table 1 provides a degree of reliability of the S−H method to produce the dimerization constant of a weakly interacting pair described by the LJ potential. To be sure, this comparison represents a favorable case consisting of rare gas atoms. On the other hand, direct experimental determinations of K_{eq} for molecular van der Waals dimers do not seem to be readily available.

RESULTS

Values of K_{eq} for N_2 and O_2 dimerization were obtained between 80−120 K. This range was chosen to include the reduced temperature of $T_r = 0.7$ of each gas (i.e., $0.7T_c$, where T_c is the critical temperature) to enable comparisons to be made with other nonpolar gases, as described in ref 6, as discussed below. For N_2 and O_2, these temperatures are 88.33 and 108.21 K, respectively.

The enthalpy and entropy changes for dimerization eqs 1 and 3 were calculated from the following relations.

https://doi.org/10.1021/acs.jpca.3c04809
J. Phys. Chem. A XXXX, XXX, XXX−XXX

$$\Delta H = RT^2\left(\frac{\mathrm{d}\ln K_{eq}}{\mathrm{d}T}\right) \text{ and } \Delta S = R\left(T\frac{\mathrm{d}\ln K_{eq}}{\mathrm{d}T} + \ln K_{eq}\right) \quad (4)$$

We present in Table 2 the values of K_{eq}, ΔH, and ΔS between 80 and 120 K for the formation of $(N_2)_2$ and $(O_2)_2$ and the $(N_2)(O_2)$. For the homodimer calculations, two sets of K_{eq}, ΔH, and ΔS were calculated using each of the LJ parameters mentioned above.[26,27] Table 2 contains the averages of the respective quantities. Their uncertainties are estimated from the respective standard deviations. Similarly, the values and estimated uncertainties for the heterodimer were obtained in the same way from the six different calculations (two sets of LJ parameters and three combining rules). An expanded table is available in the SI.

The larger relative uncertainty in K_{eq} for N_2 dimerization relates to the larger relative differences in the chosen set of LJ parameters[26,27] for N_2 than for O_2 (see Table S1 of the SI). From Table 2, it can be seen that the K_{eq} values of $(N_2)(O_2)$ are larger than those for both $(N_2)(N_2)$ and $(O_2)(O_2)$. This difference is due, in part, to the fact that symmetry number 2 is included in the S−H calculation of homodimer equilibrium. As pointed out in ref 23, a factor of 2 must, then, be applied to the calculation of K_{eq} for the heterodimer.

It is also noted that for the three dimers, ΔH becomes more negative with increasing temperature, indicating that $\Delta C_P < 0$, largely because of the decrease in translational heat capacity associated with dimerization (eqs 1 and 3). It is shown in the SI that $\Delta C_P = C_{P,D,int} - 2C_{P,M,int} - 2.5R$, where $C_{P,D,int}$ and $C_{P,M,int}$ are the respective internal (rotational−vibrational) heat capacities of the dimer and the monomer. Furthermore, at sufficiently low temperatures and for diatomic monomers, $C_{P,D,int} - 2C_{P,M,int} \simeq C_{P,D,vib,vdW} - R/2$, in which $C_{P,D,vib,vdW}$ is the heat capacity of the dimer contributed by the four low-frequency van der Waals vibrations.

Table 2. Values of K_{eq}, ΔH, and ΔS For the Dimers $(N_2)(N_2)$, $(O_2)(O_2)$, and $(N_2)(O_2)$ between 80 and 120 K

T/K	species[a]	K_{eq}[b]	ΔH[c]	ΔS[d]
80	A	0.03379	−1914	−52.10
	B	0.04116	−2000	−51.53
	C	0.07933	−2093	−47.17
84	A	0.02938	−1900	−53.03
	B	0.03557	−2072	−52.41
	C	0.06815	−2156	−47.95
88	A	0.02576	−2060	−53.85
	B	0.03103	−2137	−53.16
	C	0.05916	−2212	−48.60
92	A	0.02275	−2132	−54.64
	B	0.02728	−2204	−53.91
	C	0.05180	−2272	−49.26
96	A	0.02021	−2205	−55.42
	B	0.02415	−2274	−54.64
	C	0.04571	−2336	−49.93
100	A	0.01807	−2279	−56.18
	B	0.02151	−2344	−55.37
	C	0.04061	−2401	−50.60
104	A	0.01623	−2354	−56.91
	B	0.01927	−2417	−56.07
	C	0.03630	−2469	−51.26
108	A	0.01465	−2430	−57.63
	B	0.01735	−2490	−56.76
	C	0.03262	−2538	−51.91
112	A	0.01328	−2507	−58.32
	B	0.01569	−2564	−57.44
	C	0.02946	−2609	−52.55
116	A	0.01209	−2584	−59.00
	B	0.01425	−2639	−58.10
	C	0.02672	−2680	−53.18
120	A	0.01104	−2658	−59.62
	B	0.01299	−2710	−58.70
	C	0.02433	−2748	−53.76

[a]Rows labeled A, B, and C contain values for $(N_2)(N_2)$, $(O_2)(O_2)$, and $(N_2)(O_2)$, respectively. [b]Average percent uncertainties are 7.5 for $(N_2)(N_2)$, 3.2 for $(O_2)(O_2)$, and 4.1 for $(N_2)(O_2)$. [c]J/mol. Average percent uncertainties are 0.060 for $(N_2)(N_2)$, 0.28 for $(O_2)(O_2)$, and 0.22 for $(N_2)(O_2)$. [d]J/mol-K. Average percent uncertainties are 1.2 for $(N_2)(N_2)$, 0.58 for $(O_2)(O_2)$, and 0.64 for $(N_2)(O_2)$.

Table 3. Average Values of ΔC_P, ΔS_{trans}, and $S_{D,int}$ between 80−120 K for the Dimerization Equilibria[a]

dimer	$\langle\Delta C_P\rangle$	$\langle\Delta S_{trans}\rangle$[b]	$\langle S_{D,int}\rangle$[c]
$(N_2)(N_2)$	−18.6	−118.9	126.8
$(O_2)(O_2)$	−17.7	−120.6	134.8
$(N_2)(O_2)$	−16.4	−119.7	135.9

[a]Values in J/mol-K. [b]Change in translational entropy. [c]Internal (rotational−vibrational) entropy of the dimer.

Similarly, the negative values of ΔS shown in Table 2 arise mainly from the loss of translational entropy in the formation of the dimers from the monomers. It is shown in the SI that the rotational−vibrational entropies of the dimers can be calculated from ΔS and the monomer entropies. Table 3 contains the average values of these quantities for the three dimers between 80 and 120 K.

The data in Table 2 are portrayed graphically in Figure 1, which shows plots of $\ln K_{eq}$ vs $1/T$. The curvature shown by each, reflecting the temperature dependence of the ΔH values shown in Table 2, suggests that, aside from $\Delta C_P < 0$, monomer−dimer equilibrium involves more than one thermodynamically distinguishable dimer, as shown by the different equilibrium structures of the dimers (Figure 1). Accordingly, ΔH and ΔS also contain contributions stemming from the structural forms of the dimers.

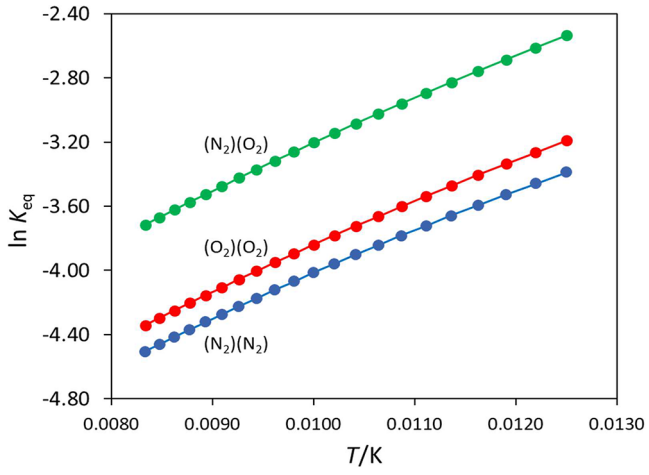

Figure 2. Plots of $\ln K_{eq}$ vs $1/T$ for the three dimers between 80 and 120 K. Dots are calculated values. Curves are second-order regression fits to the data. —— $(N_2)(N_2)$; —— $(O_2)(O_2)$; —— $(N_2)(O_2)$.

https://doi.org/10.1021/acs.jpca.3c04809
J. Phys. Chem. A XXXX, XXX, XXX−XXX

The vertical displacement of the curves illustrates the ordering of equilibrium constants shown in Table 2, i.e., $K_{eq(N_2)(O_2)} > K_{eq(O_2)(O_2)} > K_{eq(N_2)(N_2)}$. The smooth curves in Figure 2 show the respective second-order regression fits. The regression parameters are contained in the SI (Figure 2).

It is worthwhile to consider how the ΔH values of the $(N_2)(N_2)$ and $(O_2)(O_2)$ equilibria compare to those of other van der Waals dimers formed from nonpolar molecules. In ref 6, a correlation was demonstrated between ΔH for 15 species (5 rare gases and 10 nonpolar molecules), each obtained at the reduced temperature of $T_r = 0.7$, and their respective LJ well depths (determined from critical temperatures and acentric factors). Applying that correlation[6] to the formation of $(N_2)(N_2)$ and $(O_2)(O_2)$, one obtains $\Delta H = -2055(86)$ and $-2541(108)$, which compares with the S−H values of $-2066(8)$ and $-2500(13)$ J/mol at 88.34 and 108.21 K, respectively. The agreement between the S−H and correlated ΔH_D values being within the range of uncertainty of the correlation function for both dimers lends credence to the S−H method.

There are few reports of experimental determinations of the energetic, structural, or spectroscopic properties of the $(N_2)(N_2)$ and $(O_2)(O_2)$ van der Waals dimers.[32−38] In a 1924 paper, Lewis interpreted the decrease in the specific magnetic susceptibility of liquid oxygen with increasing dilution by liquid nitrogen between 64 and 77 K as being due to the equilibrium between a diamagnetic species, "the molecule O_4," and O_2.[32]

From the IR absorption spectrum of high-pressure gaseous oxygen, Salow and Steiner assigned the presence of a "loosely bound O_4 molecule" on the basis of the second-order dependence of the IR band absorption intensity on oxygen pressure.[33] Data from a similar study of high-pressure oxygen, reported by Long and Ewing between 87−110 K, yields $\Delta H = -2910(300)$ J/mol.[35] The S−H value, averaged over this temperature range, is $-2337(7)$ J/mol. In contrast to these values, Pfeilsticker et al. report the average value of the ΔH value to be $-1207(83)$ J/mol between 203 and 250 K based on the differential absorption of seven ultraviolet/visible absorption bands under atmospheric conditions.[38] Considering that $\Delta C_P < 0$, one expects ΔH to be significantly more negative at these higher temperatures relative to the value of Long and Ewing. We have no explanation for this difference.

Composition of $(N_2)(N_2)$, $(O_2)(O_2)$, and $(N_2)(O_2)$ in Earth's Atmosphere. The mole fraction composition profiles of the $(N_2)(N_2)$, $(O_2)(O_2)$, and $(N_2)(O_2)$ dimers were calculated from the respective K_{eq} values between 215−290 K, the temperature range of the troposphere and lower stratosphere, i.e., for altitudes up to 20 km. For this purpose, we obtained K_{eq} using the S−H method, as described below. This method produces K_{eq} over a specified temperature range.

The P, T, z relations given in ref 39 for the troposphere ($0 < z < 11$ km) and the tropopause/lower stratosphere ($11 < z < 20$ km) were adapted to enable one to express the altitude z (in km) and the atmospheric pressure P_{atm} (in bars) as functions of T. Thus, for the troposphere,

$$z/\text{km} = c_1 - c_2 T \tag{5}$$

$$P_{atm}/\text{bar} = c_3 T^{c_4} \tag{6}$$

where $c_1 = 44.337$ km, $c_2 = 0.15385$ km/K, $c_3 = 1.19576 \times 10^{-13}$ bar/K$^{-c_4}$, and $c_4 = 5.256$.

In the tropopause and lower stratosphere ($11 < z < 20$ km), the temperature is presumed constant at 216.69 K,[39] and P_{atm} decreases exponentially with altitude, as

$$P_{atm}/\text{bar} = c_5 \exp(-c_6 z) \tag{7}$$

in which $c_5 = 1.123$ bar and $c_6 = 1.73$ km^{-1}.

The mole fractions of N_2 and O_2 in the atmosphere, $x_{N_2,atm}$ and $x_{O_2,atm}$, are taken as $x_{N_2,atm} = 0.78084$ and $x_{O_2,atm} = 0.20947$, respectively,[40] and are assumed to be constant in the altitude range considered (the mole fraction data cited in ref 40 do not account for water vapor). The dimer partial pressure was calculated from the respective K_{eq} value to be

$$P_D \cong K_{eq}(P_A)(P_B) \tag{8}$$

in which $P_A = P_B$ is the atmospheric partial pressure of N_2 (or O_2) for the homodimers. For the $(N_2)(O_2)$ heterodimer, $P_A = P_{N_2}$ and $P_B = P_{O_2}$. The partial pressures of N_2 and O_2 in the atmosphere are given by

$$P_{N_2} = x_{N_2} P_{atm} \quad \text{and} \quad P_{O_2} = x_{O_2} P_{atm} \tag{9}$$

where P_{atm} is the atmospheric pressure.

The validity of eq 8 follows from the fact that $K_D \ll 1$ for all dimers and thus $P_D \ll P_A, P_B$. The mole fraction of dimer in the atmosphere, $x_{D,atm}$, is given by P_D/P_{atm} and can be expressed, using eqs 8 and 9, as

$$x_{D,atm} = K_{eq} x_A x_B P_{atm} \tag{10}$$

Note that in eq 10, both K_{eq} and P_{atm} are temperature-dependent. Equation 10 is used to calculate the altitude profiles of $x_{(N_2)(N_2)}$, $x_{(O_2)(O_2)}$, and $x_{(N_2)(O_2)}$. The results are shown numerically in Table 4 and graphically in Figure 3, as $\log_{10} x_D$ vs z.

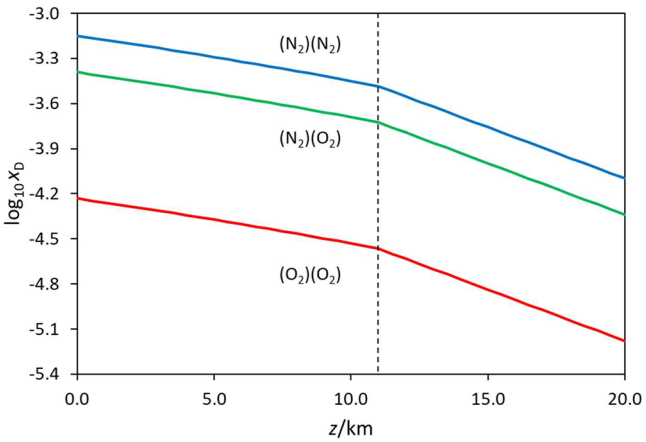

Figure 3. Log_{10} of the atmospheric mole fractions of $(N_2)(N_2)$ (——), $(O_2)(O_2)$ (——), and $(N_2)(O_2)$ (——) vs altitude. The vertical dashed line marks the transition from the troposphere to the tropopause.

From Figure 3, it can be seen that at tropospheric altitudes ($z < 11$ km), the dimer mole fractions decrease with altitude more gradually than at the higher altitudes, between 11 and 20 km. From eq 10, this can be seen to be the result of two opposing effects: the decrease in P_{atm} with increasing altitude and the increase in K_{eq} (the latter arising from the decrease in temperature). The steeper decrease in x_D for $z > 11$ km marks the transition to the constant-temperature tropopause/lower

https://doi.org/10.1021/acs.jpca.3c04809
J. Phys. Chem. A XXXX, XXX, XXX−XXX

Table 4. Altitude Profiles of the Temperature, Pressure, and Mole Fractions of $(N_2)(N_2)$, $(O_2)(O_2)$, and $(N_2)(O_2)$ in the Atmosphere Up to 20 km[a,b]

			$x_{(N_2)(N_2)} \times 10^4$		$x_{(O_2)(O_2)} \times 10^4$		$x_{(N_2)(O_2)} \times 10^4$	
z/km	T/K	P_{atm}/bar	a	b	a	b	a	b
0.0	288.19	1.013	7.09(44)	0.076	0.587(17)	0.0025	4.062(14)	0.0081
1.0	281.69	0.8987	6.66(42)		0.552(16)		3.82(13)	
2.0	275.19	0.7950	6.25(39)		0.518(15)		3.59(12)	
3.0	268.69	0.7011	5.86(37)		0.486(14)		3.36(12)	
4.0	262.19	0.6164	5.48(34)		0.455(13)		3.15(11)	
5.0	255.69	0.5402	5.12(32)		0.425(12)		2.94(10)	
6.0	249.19	0.4719	4.78(30)		0.396(12)		2.74(10)	
7.0	242.69	0.4106	4.45(28)		0.369(11)		2.55(9)	
8.0	236.19	0.3561	4.13(26)		0.343(10)		2.37(8)	
9.0	229.69	0.3075	3.83(24)		0.318(9)		2.20(8)	
10.0	223.19	0.2644	3.54(22)	0.045	0.294(9)	0.0015	2.04(7)	0.0048
11.0	216.69	0.2264	3.28(20)		0.272(8)		1.88(7)	
12.0	216.69	0.1935	2.80(18)		0.2326(7)		1.61(6)	
13.0	216.69	0.1654	2.392(15)		0.199(7)		1.438(5)	
14.0	216.69	0.1413	2.04(13)		0.4170(5)		1.18(4)	
15.0	216.69	0.1208	1.75(11)		0.145(4)		1.01(3)	
16.0	216.69	0.1032	1.49(9)		0.124(4)		0.860(30)	
17.0	216.69	0.08825	1.28(8)		0.106(3)		0.735(25)	
18.0	216.69	0.07543	1.09(1)		0.0907(26)		0.628(22)	
19.0	216.69	0.06447	0.933(58)		0.0775(23)		0.537(19)	
20.0	216.69	0.05510	0.797(50)	0.010	0.0663(19)	0.00035	0.459(16)	0.0011

[a]This work. [b]Reference 20.

stratosphere, with constant K_{eq} values and the exponential decrease in P_{atm} (see eq 7).

Previous calculations of the mole fraction profiles, based on mp4/6-31+g* calculations that include basis set superposition (BSSE) adjustments, have been reported by Slanina et al.[20] However, our results differ from theirs, being larger for the $(N_2)(N_2)$, $(O_2)(O_2)$, and $(N_2)(O_2)$ dimers by factors of ca. 70, 120, and 180 at 0, 10, and 20 km, respectively, (see Table 2). It is not possible to explain these discrepancies since no information about the underlying calculations of the data (e.g., calculations of K_{eq}) in ref 20 was provided. However, the authors of ref 20 state that the data reported is a "lower bound of the dimeric populations." Furthermore, it is reported that the mole fractions of the N_2 and O_2 dimers at 298 K and 1 atm pressure are 0.086 and 0.016, respectively, for the same calculations but without the BSSE adjustment.[20]

To place the results of Table 4 in context, we show in Table 5 our calculated dimer mole fractions, averaged over the altitude range 0 to 20 km, along with the compositions of other atmospheric gases (not including water vapor). It is evident that the three dimers rank fifth and seventh in abundance, below CO_2 and above Ne. Although their role in atmospheric chemistry or energy transfer processes is not clear, it is appropriate that they be considered in the inventory of gases in the Earth's atmosphere.

The presence and possible role of water dimers in Earth's atmosphere have been reported.[41−43] The composition of these dimers at a given altitude depends on the partial pressure of water. It is expected that K_{eq} for water is larger than those for van der Waals dimers formed from nonpolar monomers. From the data reported by Ruscic,[44] K_{eq} for the dimerization of H_2O is 0.0670 at 285 K, which compares with 9.55×10^{-4} and 1.10×10^{-3} for the N_2 and O_2 at that temperature.

Table 5. Mole Fractions of Atmospheric Gases, Including $(N_2)(N_2)$, $(O_2)(O_2)$, and $(N_2)(O_2)$[a,b]

gas	$x_D \times 10^4$
N_2	7808.4
O_2	2094.7
Ar	93.4
CO_2	3.5
$(N_2)(N_2)$	3.4(2)[c]
$(N_2)(O_2)$	2.0(1)[c]
$(O_2)(O_2)$	0.28(1)[c]
Ne	0.1818
He	0.00524
CH_4	0.00170
Kr	0.00114
H_2	5.3×10^{-3}
N_2O	3.1×10^{-3}
CO	1.0×10^{-3}
Xe	9×10^{-4}
O_3	7×10^{-4}
NO_2	2×10^{-4}

[a]Not including water vapor. [b]Values for gases other than dimers (ref 40) are assumed to be invariant with altitude. [c]Average of the values in Table 4.

CONCLUSIONS

Like other nonpolar molecules, N_2 and O_2 molecules form weakly bound van der Waals dimers that exist in several structural forms. The equilibrium constants and related thermophysical quantities of dimer formation, including the heterodimer $(N_2)(O_2)$, can be calculated from the second virial coefficients of N_2 and O_2 obtained from Lennard-Jones pair potentials using the statistical thermodynamic method described by Stogryn and Hirschfelder.[23,24] The enthalpies of formation of the N_2 and O_2 dimers are consistent with those of

https://doi.org/10.1021/acs.jpca.3c04809
J. Phys. Chem. A XXXX, XXX, XXX−XXX

other nonpolar molecules found from equation of state-based calculations. These calculations show that the three dimers rank fifth to seventh in abundance between CO_2 and Ne in the troposphere and the lower stratosphere (up to 20 km).

■ ASSOCIATED CONTENT

Supporting Information

The Supporting Information is available free of charge at https://pubs.acs.org/doi/10.1021/acs.jpca.3c04809.

LJ parameters and combining rules; examples and applications of the S−H method, and regression parameters for fitting functions in Figure 2 (PDF)

■ AUTHOR INFORMATION

Corresponding Author

Arthur M. Halpern − *Department of Chemistry and Physics, Indiana State University, Terre Haute, Indiana 47809, United States;* orcid.org/0000-0002-2211-2826; Email: Arthur.Halpern@indstate.edu

Complete contact information is available at: https://pubs.acs.org/10.1021/acs.jpca.3c04809

Notes

The author declares no competing financial interest.

■ ACKNOWLEDGMENTS

The author declares no financial support. The author is grateful to Prof. L. M. Raff for helpful discussions and to a reviewer for constructive comments.

■ REFERENCES

(1) Ewing, G. E. Intermolecular Interactions: van der Waals Molecules. *Angew. Chem., Int. Ed.* **1972**, *11* (6), 486−495.

(2) Halpern, A. M. Equilibrium state thermodynamic properties of rare gas dimers and trimers obtained from equation of state and statistical thermodynamics: application to neon, argon, krypton and xenon. *J. Chem. Thermodyn.* **2021**, *162*, No. 106558.

(3) Halpern, A. M. Thermodynamics of Helium-4 Dimerization and Trimerization. *J. Phys. Chem. A* **2021**, *125* (41), 9071−9076.

(4) Halpern, A. M. The thermodynamics of the van der Waals dimer and trimer formation in gaseous carbon dioxide and methane and their heterodimers. *J. Chem. Thermodyn.* **2022**, *172*, No. 106818.

(5) Halpern, A. M. Thermodynamics of the dimers and trimers of H_2 and D_2 and their heterodimer $(H_2)(D_2)$. *ACS Phys. Chem. Au* **2022**, *2*, 346−352.

(6) Halpern, A. M. Thermodynamic properties of van der Waals dimers and trimers of nonpolar gases and their correlation with Lennard-Jones potential well depths. *J. Phys. Chem. A* **2023**, *127* (7), 1628−1635.

(7) Tennyson, J.; van der Avoird, A. Quantum dynamics of the van der Waals molecule $(N_2)_2$ An ab initio treatment. *J. Chem. Phys.* **1982**, *77* (11), 5664−5681.

(8) Uhlik, F.; Slanina, Z.; Hinchcliffe, A. Computational studies of atmospheric chemistry species part VI. An ab initio correlated study of structure, energetics and vibrations of nitrogen dimer $(N_2)_2$. *J. Mol. Struct.* **1993**, *101* (3), 271−275.

(9) Uhlik, F.; Slanina, Z.; Hinchcliffe, A. Computed gas-phase thermodynamics of nitrogen (N_2) association. *Thermochim. Acta* **1994**, *223* (1−2), 1−6.

(10) Couronne, O.; Ellinger, Y. An ab initio and DFT study of $(N_2)_2$ dimers. *Chem. Phys. Lett.* **1999**, *306*, 71−77.

(11) Aquilanti, V.; Bartolomai, M.; Cappelletti, D.; Carmona-Novillo, E.; Pirani, F. The $N_2 - N_2$ system: An experimental potential energy surface and calculated rotovibrational levels of the molecular nitrogen dimer. *J. Chem. Phys.* **2002**, *117* (2), 615−627.

(12) Jafari, A. H. K.; Maghari, A.; Shahbazian, S. An improved ab initio potential energy surface for N_2−N_2. *Chem. Phys.* **2005**, *314*, 249−262.

(13) Gomez, L.; Bussery-Honvault, B.; Cauchy, T.; Bartolomi, M.; Cappelletti, D.; Pirani, F. Global fits of new intermolecular ground state potential energy surfaces for N_2−H_2 and N_2−N_2 van der Waals dimers. *Chem. Phys. Lett.* **2007**, *445*, 99−107.

(14) Uhlik, F.; Slanina, Z.; Hinchcliffe, A. Computational studies of atmospheric chemistry species part XIII. An ab initio correlated study of structure, energetics and vibrations of $(O_2)_2$. *J. Mol. Struct.: THEOCHEM* **1993**, *104* (3), 273−276.

(15) Aquilanti, V.; Ascenzi, D.; Bartolomei, M.; Cappelletti, D.; Cavalli, S.; de Castro Vitores, M.; Pirani, F. Molecular Beam Scattering of Aligned Oxygen Molecules. The Nature of the Bond in the O_2—O_2 Dimer. *J. Am. Chem. Soc.* **1999**, *121* (46), 10794−10802.

(16) Hernandez-Lamoneda, R.; Bartolomei, M.; Hernandez, M. I.; Campos-Martinez, J.; Dayou, F. Intermolecular potential of the O_2—O_2 Dimer. An ab Initio study and comparison with experiment. *J. Phys. Chem. A* **2005**, *50*, 11587−11595.

(17) Bartolomei, M.; Hernandez, M. I.; Campos-Martinez, J.; Carmona-Novillo, E.; Hernandez-Lamoneda, R. The intermolecular potentials of the O_2—O_2 dimer: a detailed ab initio study of the energy splittings for the three lowest multiplet states. *Phys. Chem. Chem. Phys.* **2008**, *10*, 5374−5380.

(18) Uhlik, F.; Slanina, Z.; De Almeida, W. B. Computed gas-phase thermodynamics of the N_2—O_2 complexes. *Thermochim. Acta* **1993**, *225* (1), 1−7.

(19) De Almeida, W.; Slanina, Z. Computational studies of atmospheric chemistry species. Part 7. An ab initio study of the N_2···O_2 heterodimer. *J. Mol. Struct.: THEOCHEM* **1993**, *104* (1), 77−87.

(20) Slanina, Z.; Uhlik, F.; De Almeida, W. D.; Hinchcliffe, A. A computational thermodynamic evaluation of the altitude profiles of $(N_2)_2$, N_2—O_2 and $(O_2)_2$ in the Earth's atmosphere. *Thermochim. Acta* **1994**, *231* (1−2), 55−60.

(21) Aquilanti, V.; Bartolomei, M.; Cappelletti, D.; Carmona-Novillo, E.; Pirani, F. Dimers of the major components of the atmosphere: Realistic potential energy surfaces and quantum mechanical prediction of spectral features. *Phys. Chem. Chem. Phys.* **2001**, *3* (18), 3891−3894.

(22) Aquilanti, V.; Bartolomei, M.; Carmona-Novillo, E.; Pirani, F. The asymmetric dimer N2−O2: Characterization of the potential energy surface and quantum mechanical calculation of rotovibrational levels. *J. Chem. Phys.* **2003**, *118*, 2214−2222.

(23) Stogryn, D. E.; Hirschfelder, J. O. Contributions of Bound, Metastable, and Free Molecules to the Second Virial Coefficient and Some Properties of Double Molecules. *J. Chem. Phys.* **1959**, *31* (6), 1531−1545.

(24) Stogryn, D. E.; Hirschfelder, J. O. Errata: "Contributions of Bound, Metastable, and Free Molecules to the Second Virial Coefficient and Some Properties of Double Molecules" and "Initial Pressure Dependence of Thermal Conductivity and Viscosity". *J. Chem. Phys.* **1960**, *33*, 942−943.

(25) Frurip, D. J.; Curtiss, L. A.; Blander, M. Characterization of Molecular Association on Acetone Vapor. Thermal Conductivity Measurements and Molecular orbital Calculations. *J. Phys. Chem. A* **1978**, *82* (24), 2555−2561.

(26) Hirschfelder, J. O.; Curtiss, C. F.; Bird, R. B. *Molecular Theory of Gases and Liquids*; John Wiley & Sons, Inc.: New York, 1954; p 1111.

(27) Cuadros, F.; Cachadiña, I.; Ahumada, W. Determination of Lennard-Jones Interaction Parameters Using a New Procedure. *Mol. Eng.* **1996**, *6*, 319−325.

(28) Kong, C. L. Combining rules for intermolecular potential parameters. II. Rules for the Lennard-Jones (12−6) potential and the Morse potential. *J. Chem. Phys.* **1973**, *59*, 2464−2467.

(29) Waldman, M.; Hagler, A. T. New combining rules for rare gas van der Waals parameters. *J. Comput. Chem.* **1993**, *14* (9), 1077−1084.

(30) Milne, T. A.; Vandegrift, A. E.; Greene, F. T. Mass-Spectrometric Observations of Argon Clusters in Nozzle Beams II. The Kinetics of Dimer Growth. *J. Chem. Phys.* **1970**, *52* (3), 1552−1560.

(31) Milne, T. A.; Greene, F. T. Mass-Spectrometric Observations of Argon Clusters in Nozzle Beams I. General Behavior and Equilibrium Dimer. *J. Chem. Phys.* **1967**, *47* (10), 4095−4101.
(32) Lewis, G. N. The magnetism of oxygen and the molecule O_4. *J. Am. Chem. Soc.* **1924**, *46*, 2027−2032.
(33) Salow, H.; Steiner, W. Absorption Spectrum of Oxygen at High Pressures and the Existence of the O_4 Molecule. *Nature* **1934**, *134*, No. 463.
(34) Long, C. A.; Ewing, G. E. Spectroscopic investigation of van der Waals molecules. I. The infrared and visible spectra of $(O_2)_2$. *J. Chem. Phys.* **1973**, *58* (11), 4824−4834.
(35) Long, C. A.; Ewing, G. E. The infrared spectrum of bound state oxygen dimers in the gas phase. *Chem. Phys. Lett.* **1971**, *9* (3), 225−229.
(36) Long, C. A.; Henderson, G.; Ewing, G. E. The infrared and visible spectrum of $(N_2)_2$ van der Waals molecule. *Chem. Phys.* **1973**, *2*, 485−489.
(37) Brocks, G.; van der Avoird, A. Infrared spectra of the van der Waals molecule $(N_2)_2$. *Mol. Phys.* **1985**, *55* (1), 11−32.
(38) Pfeilsticker, K.; Bösch, H.; Camy-Peyret, C.; Fitzenberger, R.; Harder, H.; Osterkamp, H. First Atmospheric Measurements of UV/visible O_4 Absorption Band Intensities: Implications for the Spectroscopy, and the Formation Enthalpy of the $O_2−O_2$ Dimer. *Geophys. Res. Lett.* **2001**, *28* (24), 4595−4598.
(39) Earth Atmosphere Model, 2023. https://www.grc.nasa.gov/WWW/K-12/airplane/atmosmet.html. (accessed Oct, 2023).
(40) Introduction to the Atmosphere, 2023. https://www.noaa.gov/jetstream/atmosphere. (accessed Oct, 2023).
(41) Gebbie, H. A.; Burroughs, W. J.; Chamberlain, J.; Harries, J. E.; Jones, R. G. Dimers of the Water Molecule in the Earth's Atmosphere. *Nature* **1969**, *221*, 143−145.
(42) Tretyakov, M. Yu.; Seroc, E. A.; Koshelec, M. A.; Parshin, V. V.; Krupnov, A. F. Water Dimer Rotationally Resolved Millimeter-Wave Spectrum Observation at Room Temperature. *Phys. Rev. Lett.* **2013**, *110*, No. 093001.
(43) Anglada, J. M.; Soléb, A. Impact of the water dimer on the atmospheric reactivity of carbonyl oxides. *Phys. Chem. Chem. Phys.* **2016**, *18*, 17698−17712.
(44) Ruscic, B. Active thermochemical Tables: Water and Water Dimer. *J. Phys. Chem. A* **2013**, *117*, 11940−11953.

https://doi.org/10.1021/acs.jpca.3c04809
J. Phys. Chem. A XXXX, XXX, XXX−XXX